Title page

Title

Extracellular matrix modulating effects of amnion-derived mesenchymal stem cells on aging skin wounds in α-Klotho knockout mice

Running head

ECM modulating effects of AMSC

Authors

Yuki Sasaki,[1] Shunsuke Ohnishi,[2] Hiroko Takahashi,[1] Kosuke Ishikawa,[1] Takahiro Miura,[1] Emi Funayama,[1] Naoto Okubo,[2] Yuhei Yamamoto[1] and Taku Maeda[1]

[1]*Department of Plastic and Reconstructive Surgery, Faculty of Medicine and Graduate School of Medicine, Hokkaido University*

[2]*Laboratory of Molecular and Cellular Medicine, Faculty of Pharmaceutical Sciences, Hokkaido University*

Correspondence: Taku Maeda MD PhD,

Department of Plastic and Reconstructive Surgery,

Faculty of Medicine and Graduate School of Medicine, Hokkaido University,

Kita 15, Nishi 7, Kita-ku, Sapporo, 060-8638, Japan; Tel: +81-11-706-6978,

Fax: +81-11-706-7827, E-mail: takumaeda1105@yellow.plala.or.jp

Abstract

Aim: Wounds in the elderly are frequently recalcitrant and chronic as a result of the effects of skin aging and associated complications. The objective of this study is to utilize α-Klotho knockout (KO) mice wound model to assess the capacity of amnion-derived mesenchymal stem cells (AMSCs) to facilitate wound healing in aging skin.

Methods: AMSCs were applied topically to the wound after extraction and gelatinization of the conditioned medium (CM). Animal experiments were performed with two distinct mouse strains: α-Klotho KO mice and wild-type mice. Full-thickness skin defect models with a diameter of 8 mm were created by incising the skin on the left and right sides of the dorsum. On day 8 after wound creation, the mice were sacrificed, and wound tissue was collected for analysis through histological and immunohistochemical evaluations, as well as quantitative polymerase chain reaction.

Results: The topical application of CM gel to wounds of α-Klotho KO mice demonstrated that wound healing was significantly higher than that observed in control, reaching the wound closure rate of wild-type mice on day 8. Additionally, gene expression analysis of wound tissue indicated that AMSC-CM may regulate extracellular matrix formation and fibrosis. Moreover, histological analysis indicated that AMSC-CM may facilitate wound contraction of aging skin wounds of α-Klotho KO mice by inducing myofibroblast differentiation and promoting granulation and collagen formation, which are the primary components of the extracellular matrix.

Conclusions: AMSC-CM may facilitate wound healing in aging skin of α-Klotho KO mice by regulating the extracellular matrix.

Keywords

extracellular matrix; klotho proteins; mesenchymal stem cells; skin aging; wound healing

Main body

Introduction

In an aging society, wounds are increasingly encountered in elderly skin.[1] Such wounds are at high risk of becoming refractory and chronic due to skin aging and various complications.[2] The development of improved treatments for aging skin wounds represents a significant challenge for plastic surgeons.

α-Klotho is a senescence-suppressing gene that was first identified in Japan in 1997.[3] Deficiency in this gene is associated with premature aging,[3] and α-Klotho knockout (KO) mice have been used in various studies as an aging model.[4,5] Previous studies on wound healing in α-Klotho KO mice have reported delayed wound healing, which is attributed to impaired re-epithelialization, collagen synthesis, and angiogenesis.[6,7] These findings largely align with the characteristics of delayed wound healing observed in aging skin.[8,9] Therefore, α-Klotho KO mice have been proposed as a useful wound healing model that reflects the characteristics of wound healing in the elderly.[6] However, studies on wound healing in α-Klotho KO mice remain limited, and further validation is required.

Mesenchymal stem cells (MSCs), which are somatic stem cells derived from mesodermal tissue, secrete a variety of bioactive substances and perform various wound healing–promoting functions.[10] These functions include regulating inflammation, promoting angiogenesis, and controlling fibrosis through paracrine effects.[11,12] MSCs can be harvested from several tissues throughout the body, including adipose tissue, bone marrow, and umbilical cord.[13-16] Our research group conducts research using amnion-derived MSCs (AMSCs), which can be harvested from the placenta following delivery.[17-25] AMSCs offer the following advantages: (1) because AMSCs can

be harvested from the placenta after cesarean section, there is no donor invasion and large volumes and high concentrations of AMSCs can be obtained; (2) AMSCs exhibit less cellular senescence and have high proliferative potential because they are of fetal origin; and (3) they are immune-privileged and therefore rejection-free, which makes allogeneic transplantation possible.[26] Accordingly, AMSC products targeting difficult-to-heal wounds have been actively developed in recent years and are attracting increasing attention.[27,28] The paracrine effects of AMSCs are thought to be mediated by bioactive substances contained in the conditioned medium (CM).[21] We have conducted studies on the effects of topically applied AMSC-CM on wound healing. As a result, it was revealed that AMSC-CM exerts fibrosis-modulating effects on keloid-derived fibroblasts, as well as anti-inflammatory and angiogenic effects in diabetic wounds.[29,30]

The objective of this study was to use the α-Klotho KO mouse wound model to ascertain the ability of topically applied AMSC-CM to promote the healing of aging skin wounds. This work may facilitate further investigation of the potential use of AMSCs as a superior therapeutic agent for refractory aging skin wounds.

Methods

Cells

Human AMSCs were kindly provided by Kaneka Corp. (Osaka, Japan). The AMSCs were confirmed to be multipotent and to express MSC markers (CD44, CD73, CD90 and CD105) but not hematopoietic markers (CD11b, CD19, CD34, CD45 and human leukocyte antigen DR).[18,22,23] Cells from the third to fourth passages were used and incubated at 37°C and 5% CO_2.[30]

Extraction of conditioned medium

AMSC-CM is obtained by collecting AMSCs incubated for a given period of time, and this procedure was performed according to our previously reported method.[30] Briefly, AMSCs are cultured until they reach sub-confluency, and then the medium is aspirated, washed, and replaced with serum-free minimal essential medium (MEM)-α (Thermo Fisher Scientific, Waltham, MA; Cat# 12571063). Because the paracrine action of MSCs is enhanced under hypoxic conditions,[31] the cells were cultured at 37°C, 1% O_2, and 5% CO_2 for 48 h, after which the CM was extracted using a 0.22-μm cell filtration filter.

Preparation of gels for topical application

To administer AMSC-CM to the wound, the extracted CM was gelatinized for topical application. As previously reported,[30] gels were prepared by dissolving carboxymethylcellulose powder (Fujifilm Wako Pure Chemical Corp., Osaka, Japan; Cat# 035-01337) in the extracted CM at a concentration of 7%. As a negative control, standard medium (SM) gels were also prepared by dissolving carboxymethylcellulose powder in serum-free MEM-α at the same concentration.

Experimental model

The animal experiments were conducted using α-Klotho KO (*kl*/*kl*; RRID: IMSR_JCL: MGM-0009) and wild-type (WT, C57BL/6JJcl; RRID:MGI:3055581) mice (male, 5 weeks old; CLEA Japan, Tokyo, Japan). Ten mice of each type were used. The mice were introduced at 4 weeks of

age and permitted a 1-week acclimation period prior to the experiments. The mice were housed in a specific pathogen-free facility under controlled environmental conditions. The temperature was maintained at 22–24°C, with a humidity level of 40–60%. The light cycle was set from 7:00 AM to 7:00 PM. The mice were provided with MF diet (Oriental Yeast Co., Ltd., Tokyo, Japan) and tap water ad libitum. In accordance with the method we previously reported,[30] full-thickness skin-defect models with a diameter of 8 mm were created by incising the skin on the left and right sides of the dorsum using a standard skin biopsy punch. The wounds were treated with CM gel or SM gel, and a transparent dressing (Tegaderm; 3M Japan, Tokyo, Japan; Cat# 16002S) was applied to prevent gel overflow and contraction of the panniculus carnosus muscle. Each wound was counted as $n = 1$. The wounds were cleaned and the gel was reapplied every other day, and the wounds were photographed at each interval (EOS X2; Canon, Tokyo, Japan; Cat# 2754B001). The mice were euthanized 8 days after wound creation, and the wound tissue was collected for analysis (Fig. 1). The collected wound tissues were divided into the following groups according to the type of mouse and the externally applied gel: WT mice + SM gel group (WT + SM), α-Klotho KO mice + SM gel group (KO + SM), and α-Klotho KO mice + CM gel group (KO + CM). WT mice + CM gel group was excluded for the following reasons: The primary objective of this study was to evaluate the effect of CM gel on KO mice, not on WT mice. Since the application of CM gel in WT mice would clearly enhance wound healing, we considered its impact on the overall experimental results to be minimal. Additionally, excluding this group helped to avoid unnecessary complexity in data presentation.

α-Klotho KO mice have shortened life spans due to the early aging

phenomenon and heightened susceptibility to external stressors.[3,6] Consequently, the mice were treated with the utmost care and affection and were kept warm during and after surgery to prevent hypothermia. In addition, inhalation anesthetics were used judiciously throughout the experiment.

Evaluation of wound closure rate

The wound area was measured from macrophotographs of the wound site in each group, using ImageJ (National Institutes of Health, Bethesda, MD; RRID: SCR_003070). By comparing the remaining wound area at each time point with the initial wound area, we calculated the wound closure rate over time and analyzed the macroscopic progress of wound healing. The wound closure rate was calculated as follows:[30]

$$\text{Wound closure rate} = \left(1 - \frac{\text{remaining wound area}}{\text{initial wound area}}\right) \times 100$$

Histology and immunohistochemistry

The collected wound tissues were fixed with 4% paraformaldehyde (Fujifilm Wako Pure Chemical Corp.) and subsequently paraffin-embedded for hematoxylin and eosin (H&E) staining, Masson’s trichrome staining, and immunohistochemical staining. Sections (4 μm thick) were incubated with a monoclonal mouse anti-human smooth muscle actin antibody (Dako Cytomation, Carpinteria, CA; Cat# M0851, RRID: AB_2223500). Digital images of the slides were created using a whole-slide scanner (NanoZoomer Digital Pathology; Hamamatsu Photonics, Hamamatsu, Japan; RRID: SCR_022537), visualized using NDP.view2 software (Hamamatsu Photonics;

RRID: SCR_025177), and analyzed with ImageJ software. For each H&E-stained specimen, the mean thickness of granulation tissue was determined in 10 randomly selected points. The degree of collagen formation was evaluated by calculating the collagen volume fraction (CVF) from Masson's trichrome staining: CVF = collagen area of the wound/total field area × 100.[32] Additionally, the mean percentage of immunopositive regions for α-smooth muscle actin (α-SMA) was calculated from 10 randomly selected regions (400× magnification).[30]

RNA isolation and quantitative polymerase chain reaction

Following the cryopreservation of the collected wound tissue, total RNA extraction from the cryopreserved tissues was performed using QIA Shredder, RNase-Free DNase Set, and RNeasy Fibrous Tissue Mini Kit (all from Qiagen, Hilden, Germany). Reverse transcription was performed to generate cDNA, using a High Capacity RNA-to-cDNA Kit (Applied Biosystems, Foster City, CA). Real-time quantitative reverse transcription-polymerase chain reaction (PCR) was performed using Power SYBR Green Master Mix (Applied Biosystems) and the StepOne- Plus Real-Time PCR System (Applied Biosystems; RRID: SCR_015805). The data were subsequently analyzed using High-Resolution Melt software (Applied Biosystems). Primer sequences are shown in Supplementary Table S1.

Statistical analysis

Data are presented as mean ± standard error. One-way analysis of variance was applied to ascertain the existence of significant discrepancies between each group. Student's *t*-test was used for comparisons between two groups,

while Tukey's post hoc test was used for multiple comparisons. The threshold for statistical significance was set at $p < 0.05$. All statistical analyses were conducted using JMP software (ver. 16.0.0; SAS Institute, Cary, NC ; RRID: SCR_022199).

Results

Wound healing in aging skin of α-Klotho KO mice after topical application of CM gel

First, we used an animal model to determine whether topical application of CM gel promotes wound healing in aging skin. Clinical photographs of representative wound sites on days 0, 2, 4, 6, and 8 following the creation of the wounds in each group are presented in Fig. 2a. Subsequently, the wound closure rate at each designated time point was calculated and graphed (Fig. 2b). The results demonstrated that the WT + SM group exhibited the highest closure rate throughout the entire observation period, while the KO + SM group demonstrated the lowest closure rate. However, the KO + CM group exhibited a higher closure rate compared with the KO + SM group throughout the observation period. The wound closure rates on day 8 were 82.3% ± 3.0% in the WT + SM group, 66.4% ± 3.9% in the KO + SM group ($p = 0.024$ versus WT + SM), and 82.2% ± 3.9% in the KO + CM group ($p = 0.99$ versus WT + SM). These findings indicate that the topical application of CM gel to wounds in α-Klotho KO mice results in greater wound contraction than SM gel and increases the wound closure rate to that of WT mice on day 8.

Analysis of wound healing-related gene expression by real-time PCR

Next, to elucidate the mechanism by which the topical application of CM gel promotes wound healing, real-time PCR was performed on wound tissue collected from mice to examine the expression of genes associated with wound healing.

No significant differences were found in the expression of genes related to inflammation, angiogenesis, and cell proliferation (Supplementary Fig. S1).

Proper extracellular matrix formation is also important for normal wound healing. Therefore, we examined matrix metalloproteinases (MMPs) and tissue inhibitors of metalloproteinases (TIMPs) as genes involved in extracellular matrix formation. Compared with the WT + SM group, the KO + SM group showed a trend toward increased expression of *Mmp3* (p = 0.091), significantly increased expression of *Mmp9* (p = 0.0086), and significantly decreased expression of *Timp1* ($p < 0.0001$). However, in the KO + CM group, the expression of *Mmp3* (p = 0.92) and *Mmp9* (p = 0.79) decreased to levels comparable to the WT + SM group, whereas the expression of *Timp1* ($p < 0.0001$) was significantly increased (Fig. 3a-c). These findings suggest that *Mmp3* and *Mmp9* are elevated and *Timp1* is decreased in aging skin wounds of α-Klotho KO mice but that treatment with CM gel can suppress the elevation in *Mmp3* and *Mmp9* and increase *Timp1*.

Next, we analyzed the expression of *Acta2*, the gene encoding α-SMA, a marker of myofibroblasts that produce collagen, which is a major component of the extracellular matrix, and *Tgfb1*, the gene encoding transforming growth factor-β1 (TGF-β1), which induces myofibroblast differentiation upstream of *Acta2*. The results showed that the expression levels of *Acta2* (p = 0.013) and *Tgfb1* (p = 0.019) were significantly

decreased in the KO + SM group compared with the WT + SM group, whereas the levels of these genes were significantly increased in the KO + CM group compared with the KO + SM group (*Acta2*, $p < 0.0001$; *Tgfb1*, $p = 0.0058$; Fig. 3d and e). These results suggest that CM gel may promote the healing of aging skin wounds of α-Klotho KO mice by regulating extracellular matrix formation and fibrosis.

Analysis of fibrosis-related proteins by histology and immunohistochemistry

Based on the findings thus far, wound healing was delayed in α-Klotho KO mice but improved to a level comparable to WT mice following the application of CM gel. To further validate the effects of CM gel on the extracellular matrix and fibrosis in aging skin wounds of α-Klotho KO mice, we conducted a histological evaluation using wound tissue from α-Klotho KO mice.

Myofibroblasts are involved in granulation and play a major role in wound healing. H&E staining showed that the granulation tissue was nonsignificantly thicker in the KO + CM group than in the KO + SM group (Supplementary Fig. 2).

To determine whether more myofibroblasts were actually induced to differentiate by CM gel, α-SMA immunostaining was performed to quantify the α-SMA-positive area within the wound area. The results showed that the positive area percentage was 2.8% ± 0.8% in the KO + SM group and 8.6% ± 1.8% in the KO + CM group, indicating that CM gel significantly induced myofibroblast differentiation ($p = 0.015$; Fig. 4).

Moreover, to measure collagen deposition in the wound area in

relation to extracellular matrix formation, Masson's trichrome staining was performed and the collagen volume fraction was calculated from the positive area. The collagen volume fraction was 8.3% ± 0.7% in the KO + SM group and 12.2% ± 1.3% in the KO + CM group, indicating that CM gel significantly enhanced collagen deposition ($p = 0.025$; Fig. 5).

These results suggest that AMSC-CM may assist wound healing in aging skin wounds of α-Klotho KO mice by inducing myofibroblast differentiation to promote granulation and formation of collagen, a major component of the extracellular matrix.

Discussion

Because cellular aging parallels human aging, normal wound healing is impaired due to a decline in various cellular activities and functions.[33,34] Some of the major possible causes of delayed wound healing in the aging skin include the following: (1) prolonged inflammation due to lower neutrophil and macrophage activity; (2) decreased neovascularization due to loss of angiogenic potential; (3) reduced cell proliferation due to decreased keratinocyte proliferation; and (4) less extracellular matrix due to decreased fibroblast function, collagen synthesis and deposition, and glycosaminoglycan synthesis.[35]

Our results suggest that the topical application of AMSC-CM may promote wound closure in α-Klotho KO mice by modulating extracellular matrix and myofibroblast formation. Although MSCs have been reported to ameliorate cellular senescence,[36,37] little attention has been paid to how they promote wound healing in aging skin. Many studies have shown multiple paracrine effects of AMSCs, including anti-inflammatory, angiogenesis-

promoting, and cell proliferation–promoting effects,[22-25,29,30] but the mechanisms are complex due to their multipotency. Here, we focused mainly on the extracellular matrix based on our real-time PCR results.

MMPs are a family of enzymes that play major roles in the early stages of tissue damage and are involved in the degradation of the extracellular matrix, including collagen, proteoglycans, and fibronectin.[38] Additionally, they have a profound impact on various biological processes, including inflammation, fibrosis, and angiogenesis.[39] However, excessively elevated MMP levels lead to excessive degradation of the extracellular matrix, which impairs wound healing.[40] In contrast, TIMPs inhibit the activity of MMPs, which are considered to play a role in preventing excessive inflammation and regulating normal wound healing by modulating extracellular matrix degradation.[41] Accordingly, the equilibrium between MMPs and TIMPs *in vivo* regulates the amount of extracellular matrix in an appropriate manner. The MMP/TIMP balance is typically maintained in normal tissues. However, this equilibrium is disrupted in refractory wounds, which impedes the wound healing process.[42]

Our results showed elevated levels of *Mmp3* and *Mmp9* but decreased levels of *Timp1* in the wounds of α-Klotho KO mice compared with those of WT mice. MMP9 is elevated while TIMP1 is diminished in chronic wounds.[43] Moreover, elevated levels of MMP9 impede wound healing by suppressing granulation and inactivating growth factors.[40] Conversely, a reduction in MMP9 overexpression facilitates collagen formation in wounds and subsequent wound healing.[44] In a model of refractory wounds in diabetic mice, there were increased MMP9 levels and decreased TIMP1 expression.[45] Moreover, the application of MSCs to wounds results in reduced MMP9 and

increased TIMP1, which facilitate the healing process.[46] The aforementioned reports corroborate our findings.

Furthermore, the expression of *Acta2* and *Tgfb1* was significantly decreased in α-Klotho KO mice compared with WT mice. However, the topical application of AMSC-CM to α-Klotho KO mice induced myofibroblast differentiation and increased collagen levels. α-SMA is a marker of myofibroblast activation and plays a pivotal role in granulation and wound healing.[47] TGF-β1 regulates myofibroblast differentiation via the Smad pathway.[48] It was previously demonstrated that the administration of MSCs to wounds in rats increases the expression of α-SMA and TGF-β1, which in turn promote the healing of the wound.[47] Therefore, AMSC-CM may facilitate the formation of the extracellular matrix and accelerate the healing of wounds by enhancing myofibroblast expression.

The formation of an adequate extracellular matrix is a crucial aspect of the proliferative phase of the wound healing process. A reduction in collagen and myofibroblast levels impedes the typical progression of wound healing. The present report illustrates that AMSC-CM may facilitate wound healing in aging skin through mechanisms such as regulation of the extracellular matrix by controlling the MMP/TIMP balance and induction of myofibroblast proliferation and collagen synthesis by promoting *Tgfb1* expression.

In this study, we evaluated the wound healing process on day 8, when wound closure was nearly complete, to analyze changes during the proliferative phase of wound healing. This decision was based on previous studies reporting that aged mice exhibit a significant delay in extracellular matrix production during the proliferative phase.[9] However, analyzing

earlier time points could reveal changes in the inflammatory phase or the early proliferative phase, which may provide further insights into the wound healing process. We consider this an important aspect to investigate in future studies.

In conclusion, the topical application of AMSC-CM facilitates wound healing in α-Klotho KO mice. The primary mechanism of this effect may be through modulation of the extracellular matrix and myofibroblasts. AMSCs may prove to be a valuable tool for promoting wound healing in aging skin.

Author contributions

YS: Writing - original draft, Methodology, Investigation, Formal analysis; SO: Writing - review and editing, Methodology, Supervision, Funding acquisition, Conceptualization; HT: Methodology, Funding acquisition; KI: Writing - review and editing, Formal analysis, Methodology, Supervision; TM: Investigation; EF: Investigation, Validation. NO: Investigation; YY: Methodology, Supervision, Conceptualization; TM: Writing - review and editing, Supervision, Project administration. All authors made substantial contributions to the manuscript and approved the final version.

Acknowledgments

This study was supported by JSPS Grant-in-Aid for Early-Career Scientists; Grant number: 21K16913.

Funding statement

This study was supported by JSPS Grant-in-Aid for Early-Career Scientists; Grant number: 21K16913. Amnion-derived mesenchymal stem cells used in this study were generously provided by Kaneka Corp. (Osaka, Japan).

Conflict of interest disclosure

The authors declare that they have no conflict of interest. However, it should be noted that amnion-derived mesenchymal stem cells used in this study were provided by Kaneka Corp. (Osaka, Japan). This support did not influence the study's design, data collection, analysis, or interpretation.

Data availability statement

The data that support the findings of our study are available from the corresponding author upon reasonable request.

Ethics approval statement

The protocols used in our study were approved by the Institutional Animal Care and Use Committee, Hokkaido University School of Medicine, and were conducted in accordance with the Guidelines for the Care and Use of Laboratory Animals, Hokkaido University.

References

1 Verdolino DV, Thomason HA, Fotticchia A, Cartmell S. Wound dressings: curbing inflammation in chronic wound healing. *Emerg Top Life Sci* 2021; **5**: 523-537.

2 Sgonc R, Gruber J. Age-related aspects of cutaneous wound healing: a mini-review. *Gerontology* 2013; **59**: 159-164.

3 Kuro-o M, Matsumura Y, Aizawa H *et al.* Mutation of the mouse *Klotho* gene leads to a syndrome resembling ageing. *Nature* 1997; **390**: 45-51.

4 Kurosu H, Yamamoto M, Clark JD *et al.* Suppression of aging in mice by the hormone Klotho. *Science* 2005; **309**: 1829-1833.

5 Ohnishi M, Razzaque MS. Dietary and genetic evidence for phosphate toxicity accelerating mammalian aging. *FASEB J* 2010; **24**: 3562-3571.

6 Yamashita K, Yotsuyanagi T, Yamauchi M, Young DM. Klotho mice: a novel wound model of aged skin. *Plast Reconstr Surg Glob Open* 2014; **2**: e101.

7 Yamauchi M, Hirohashi Y, Torigoe T *et al.* Wound healing delays in *α-Klotho*-deficient mice that have skin appearance similar to that in aged humans - Study of delayed wound healing mechanism. *Biochem Biophys Res Commun* 2016; **473**: 845-852.

8 Brem H, Tomic-Canic M, Entero H *et al.* The synergism of age and db/db genotype impairs wound healing. *Exp Gerontol* 2007; **42**: 523-531.

9 Gosain A, DiPietro LA. Aging and wound healing. *World J Surg* 2004; **28**: 321-326.

10 Hanson SE, Bentz ML, Hematti P. Mesenchymal stem cell therapy for

nonhealing cutaneous wounds. *Plast Reconstr Surg* 2010; **125**: 510-516.

11 Chen L, Tredget EE, Wu PY, Wu Y. Paracrine factors of mesenchymal stem cells recruit macrophages and endothelial lineage cells and enhance wound healing. *PLoS One* 2008; **3**: e1886.

12 Ohnishi S, Ohgushi H, Kitamura S, Nagaya N. Mesenchymal stem cells for the treatment of heart failure. *Int J Hematol* 2007; **86**: 17-21.

13 Li G, Zhang Y, Wu J *et al.* Adipose stem cells-derived exosomes modified gelatin sponge promotes bone regeneration. *Front Bioeng Biotechnol* 2023; **11**: 1096390.

14 Volkova MV, Shen N, Polyanskaya A *et al.* Tissue-oxygen-adaptation of bone marrow-derived mesenchymal stromal cells enhances their immunomodulatory and pro-angiogenic capacity, resulting in accelerated healing of chemical burns. *Int J Mol Sci* 2023; **24**.

15 Hu L, Zhou J, He Z *et al.* In situ-formed fibrin hydrogel scaffold loaded with human umbilical cord mesenchymal stem cells promotes skin wound healing. *Cell Transplant* 2023; **32**: 9636897231156215.

16 Ishikane S, Ohnishi S, Yamahara K *et al.* Allogeneic injection of fetal membrane-derived mesenchymal stem cells induces therapeutic angiogenesis in a rat model of hind limb ischemia. *Stem Cells* 2008; **26**: 2625-2633.

17 Kubo K, Ohnishi S, Hosono H *et al.* Human amnion-derived mesenchymal stem cell transplantation ameliorates liver fibrosis in rats. *Transplant Direct* 2015; **1**: e16.

18 Onishi R, Ohnishi S, Higashi R *et al.* Human amnion-derived mesenchymal stem cell transplantation ameliorates dextran sulfate

sodium-induced severe colitis in rats. *Cell Transplant* 2015; **24**: 2601-2614.

19 Ono M, Ohnishi S, Honda M *et al.* Effects of human amnion-derived mesenchymal stromal cell transplantation in rats with radiation proctitis. *Cytotherapy* 2015; **17**: 1545-1559.

20 Kawakubo K, Ohnishi S, Fujita H *et al.* Effect of fetal membrane-derived mesenchymal stem cell transplantation in rats with acute and chronic pancreatitis. *Pancreas* 2016; **45**: 707-713.

21 Miyamoto S, Ohnishi S, Onishi R *et al.* Therapeutic effects of human amnion-derived mesenchymal stem cell transplantation and conditioned medium enema in rats with trinitrobenzene sulfonic acid-induced colitis. *Am J Transl Res* 2017; **9**: 940-952.

22 Mizushima T, Ohnishi S, Hosono H *et al.* Oral administration of conditioned medium obtained from mesenchymal stem cell culture prevents subsequent stricture formation after esophageal submucosal dissection in pigs. *Gastrointest Endosc* 2017; **86**: 542-552.e541.

23 Ohara M, Ohnishi S, Hosono H *et al.* Extracellular vesicles from amnion-derived mesenchymal stem cells ameliorate hepatic inflammation and fibrosis in rats. *Stem Cells Int* 2018; **2018**: 3212643.

24 Tsuda M, Ohnishi S, Mizushima T *et al.* Preventive effect of mesenchymal stem cell culture supernatant on luminal stricture after endoscopic submucosal dissection in the rectum of pigs. *Endoscopy* 2018; **50**: 1001-1016.

25 Takamiya S, Kawabori M, Yamazaki K *et al.* Intravenous transplantation of amnion-derived mesenchymal stem cells promotes functional recovery and alleviates intestinal dysfunction after spinal

cord injury. *PLoS One* 2022; **17**: e0270606.

26 Liu QW, Huang QM, Wu HY *et al.* Characteristics and therapeutic potential of human amnion-derived stem cells. *Int J Mol Sci* 2021; **22**.

27 Zelen CM, Serena TE, Snyder RJ. A prospective, randomised comparative study of weekly versus biweekly application of dehydrated human amnion/chorion membrane allograft in the management of diabetic foot ulcers. *Int Wound J* 2014; **11**: 122-128.

28 Cooke M, Tan EK, Mandrycky C, He H, O'Connell J, Tseng SC. Comparison of cryopreserved amniotic membrane and umbilical cord tissue with dehydrated amniotic membrane/chorion tissue. *J Wound Care* 2014; **23**: 465-474, 476.

29 Sato C, Yamamoto Y, Funayama E *et al.* Conditioned medium obtained from amnion-derived mesenchymal stem cell culture prevents activation of keloid fibroblasts. *Plast Reconstr Surg* 2018; **141**: 390-398.

30 Takahashi H, Ohnishi S, Yamamoto Y *et al.* Topical application of conditioned medium from hypoxically cultured amnion-derived mesenchymal stem cells promotes wound healing in diabetic mice. *Plast Reconstr Surg* 2021; **147**: 1342-1352.

31 Gao Z, Zhang C, Peng F *et al.* Hypoxic mesenchymal stem cell-derived extracellular vesicles ameliorate renal fibrosis after ischemia-reperfusion injure by restoring CPT1A mediated fatty acid oxidation. *Stem Cell Res Ther* 2022; **13**: 191.

32 Xing Z, Yang C, He J *et al.* Cardioprotective effects of aconite in isoproterenol-induced myocardial infarction in rats. *Oxid Med Cell Longev* 2022; **2022**: 1090893.

33 Samdavid Thanapaul RJR, Shvedova M, Shin GH, Crouch J, Roh DS. Elevated skin senescence in young mice causes delayed wound healing. *Geroscience* 2022; **44**: 1871-1878.

34 Chia CW, Sherman-Baust CA, Larson SA *et al.* Age-associated expression of p21and p53 during human wound healing. *Aging Cell* 2021; **20**: e13354.

35 Thomason HA, Hardman MJ. Delayed wound healing in elderly people. *Rev Clin Gerontol* 2009; **19**: 171-184.

36 Dorronsoro A, Santiago FE, Grassi D *et al.* Mesenchymal stem cell-derived extracellular vesicles reduce senescence and extend health span in mouse models of aging. *Aging Cell* 2021; **20**: e13337.

37 Zhao X, Liu Y, Jia P *et al.* Chitosan hydrogel-loaded MSC-derived extracellular vesicles promote skin rejuvenation by ameliorating the senescence of dermal fibroblasts. *Stem Cell Res Ther* 2021; **12**: 196.

38 Hoshino Y, Osawa M, Funayama E *et al.* Therapeutic potential of the prolyl hydroxylase inhibitor roxadustat in a wouse hindlimb lymphedema model. *Lymphat Res Biol* 2023; **21**: 372-380.

39 Salonurmi T, Parikka M, Kontusaari S *et al.* Overexpression of TIMP-1 under the MMP-9 promoter interferes with wound healing in transgenic mice. *Cell Tissue Res* 2004; **315**: 27-37.

40 Shao Z, Yin T, Jiang J, He Y, Xiang T, Zhou S. Wound microenvironment self-adaptive hydrogel with efficient angiogenesis for promoting diabetic wound healing. *Bioact Mater* 2023; **20**: 561-573.

41 Lotz M, Guerne PA. Interleukin-6 induces the synthesis of tissue inhibitor of metalloproteinases-1/erythroid potentiating activity

(TIMP-1/EPA). *J Biol Chem* 1991; **266**: 2017-2020.

42 Roeb E. Matrix metalloproteinases and liver fibrosis (translational aspects). *Matrix Biol* 2018; **68-69**: 463-473.

43 Subramaniam K, Pech CM, Stacey MC, Wallace HJ. Induction of MMP-1, MMP-3 and TIMP-1 in normal dermal fibroblasts by chronic venous leg ulcer wound fluid. *Int Wound J* 2008; **5**: 79-86.

44 Castleberry SA, Almquist BD, Li W *et al.* Self-assembled wound dressings silence MMP-9 and improve diabetic wound healing in vivo. *Adv Mater* 2016; **28**: 1809-1817.

45 Liu J, Chen Z, Wang J *et al.* Encapsulation of curcumin nanoparticles with MMP9-responsive and thermos-sensitive hydrogel improves diabetic wound healing. *ACS Appl Mater Interfaces* 2018; **10**: 16315-16326.

46 Xu J, Zgheib C, Hodges MM, Caskey RC, Hu J, Liechty KW. Mesenchymal stem cells correct impaired diabetic wound healing by decreasing ECM proteolysis. *Physiol Genomics* 2017; **49**: 541-548.

47 Putra A, Alif I, Hamra N *et al.* MSC-released TGF-β regulate α-SMA expression of myofibroblast during wound healing. *J Stem Cells Regen Med* 2020; **16**: 73-79.

48 Mokoena D, Dhilip Kumar SS, Houreld NN, Abrahamse H. Role of photobiomodulation on the activation of the Smad pathway via TGF-β in wound healing. *J Photochem Photobiol B* 2018; **189**: 138-144.

Supplementary Table S1. Primer sequences.

Mouse *Acta2-forward*: 5′- GACAATGGGCTCTCTGGGCTCTCTGTA -3′

Mouse *Acta2-reverse*:5′- TTTGGCCCATTCCAACCATTA -3′

Mouse *Gapdh-forward*: 5′-TGTGTCCGTCGTGGATCTGA-3′

Mouse *Gapdh -reverse*: 5′-TTGCTGTTGAAGTCGCAGGAG-3′

Mouse *Il1b-forward*: 5′- CCAGGATGAGGACATGAGCAC-3′

Mouse *Il1b-reverse*:5′- TGTTGTTCATCTCTCGGGAGCCTGTA-3′

Mouse *Mki67-forward*: 5′- GCTCACCTGGGTCACCATCAA-3′

Mouse *Mki67-reverse*:5′- CACTACAGGCAGCTGGGATACGA-3′

Mouse *Mmp3-forward*: 5′- CCTGGGACCAGGGGATTAATGGGAG-3′

Mouse *Mmp3-reverse*: 5′- GGCCAAGTTCATGAGCAGCA-3′

Mouse *Mmp9-forward*:5′- GCCCTGGAACTCACACGACA-3′

Mouse *Mmp9-reverse*: 5′- TTGGAAACTCACACACGCCAGAAG-3′

Mouse *Pecam1-forward*: 5′- CCTCCAACAGAGCCAGCAGTA-3′

Mouse *Pecam1-reverse*:5′- CGATGACCACTCCAATGACAAC-3′

Mouse *Tgfb1-forward*: 5′- TTCAACACATCAGAGAGCTCCGAGA TG-3′

Mouse *Tgfb1-reverse*:5′- GTATCGCCAGGAATTGTTGCTGTA -3′

Mouse *Timp1-forward*:5′- TCAAAGACCTATAGTGCTGGCTGTG -3′

Mouse *Timp1-reverse*: 5′- AAAGTGACGGGCTCTCTGGGTAGTCCTC -3′

Mouse *Tnf-forward*: 5′- GCCTCTTCTCATTCCTGCTTGTG -3′

Mouse *Tnf-reverse*:5′- TGATGAGAGGGAGGCCATTTG -3′

Mouse *Vegfa-forward*: 5′- AACCCATTCCTGGCCCTGA-3′

Mouse *Vegfa-reverse*:5′- GATCCACAAAGCATGCCATGTC-3′

Figure legends

Figure 1. Schema of animal experimentation protocols. Wounds were created on the dorsum of the mice (red area), and standard medium gel (blue area), as well as amnion-derived mesenchymal stem cells conditioned medium gel (yellow area), were applied topically every other day. On day 8, the mice were sacrificed, and wound tissue was collected.

Figure 2. Evaluation of wound closure in full-thickness skin-defect models. Wounds were created on the dorsum of wild-type (WT) mice or α-Klotho knockout (KO) mice, and standard medium (SM) gel or amnion-derived mesenchymal stem cells conditioned medium (CM) gel were applied topically every other day. On day 8, the mice were sacrificed, and wound tissue was collected. (a) Clinical photographs of the wound site. Left to right showing changes over time. (Top) WT mice + SM gel group. (Center) α-Klotho KO mice + SM gel group. (Bottom) α-Klotho KO mice + CM gel group. (b) Wound closure rate. By comparing the remaining wound area at each time point with the initial wound area, we calculated the wound closure rate over time and analyzed the macroscopic progress of wound healing. Data are shown as the mean ± standard error. $n = 10$ / each, $*p < 0.05$ and $**p < 0.01$.

Figure 3. Gene expression analysis of wound tissue at 8 days after wound creation. (a-c) Expression of extracellular matrix-related genes. (d, e) Expression of myofibroblast-related genes. Data are shown as the mean ± standard error. $n = 10$ / each, $*p < 0.05$ and $**p < 0.01$ versus WT + SM.

Figure 4. Effect of amnion-derived mesenchymal stem cells conditioned

medium on the expression of α-smooth muscle actin (α-SMA) in wounds of α-Klotho KO mice. Specimens were reacted with a goat anti-α-SMA antibody. (Left) Microscopic images. (Right) α-SMA-positive areas. The mean percentage of immunopositive regions was calculated from 10 randomly selected regions (400× magnification). Data are shown as the mean ± standard error. n = 10 / each, *p < 0.05 versus KO + SM. Scale bars = 100 μm.

Figure 5. Effect of amnion-derived mesenchymal stem cells conditioned medium on collagen formation in wounds of α-Klotho KO mice by Masson's Trichrome staining. (Left) Microscopic images. (Right) Collagen volume fraction (CVF). The degree of collagen formation was evaluated by calculating the CVF from Masson's trichrome staining: CVF = collagen area of the wound/total field area × 100. Data are shown as the mean ± standard error. n = 10 / each, *p < 0.05 versus KO + SM. Scale bars = 100 μm.

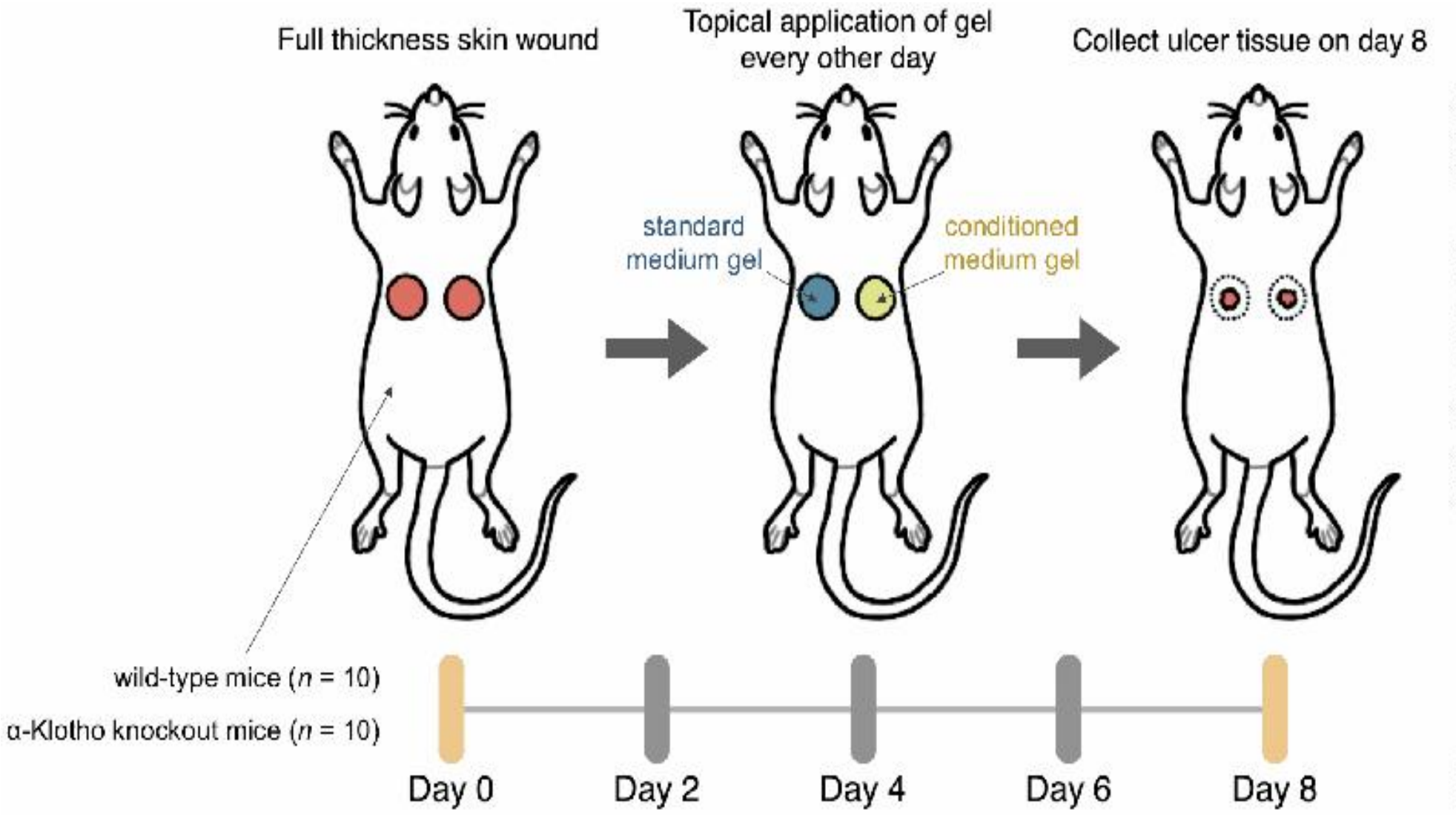
Full thickness skin wound
Topical application of gel every other day
Collect ulcer tissue on day 8
standard medium gel
conditioned medium gel
wild-type mice (n = 10)
α-Klotho knockout mice (n = 10)
Day 0
Day 2
Day 4
Day 6
Day 8

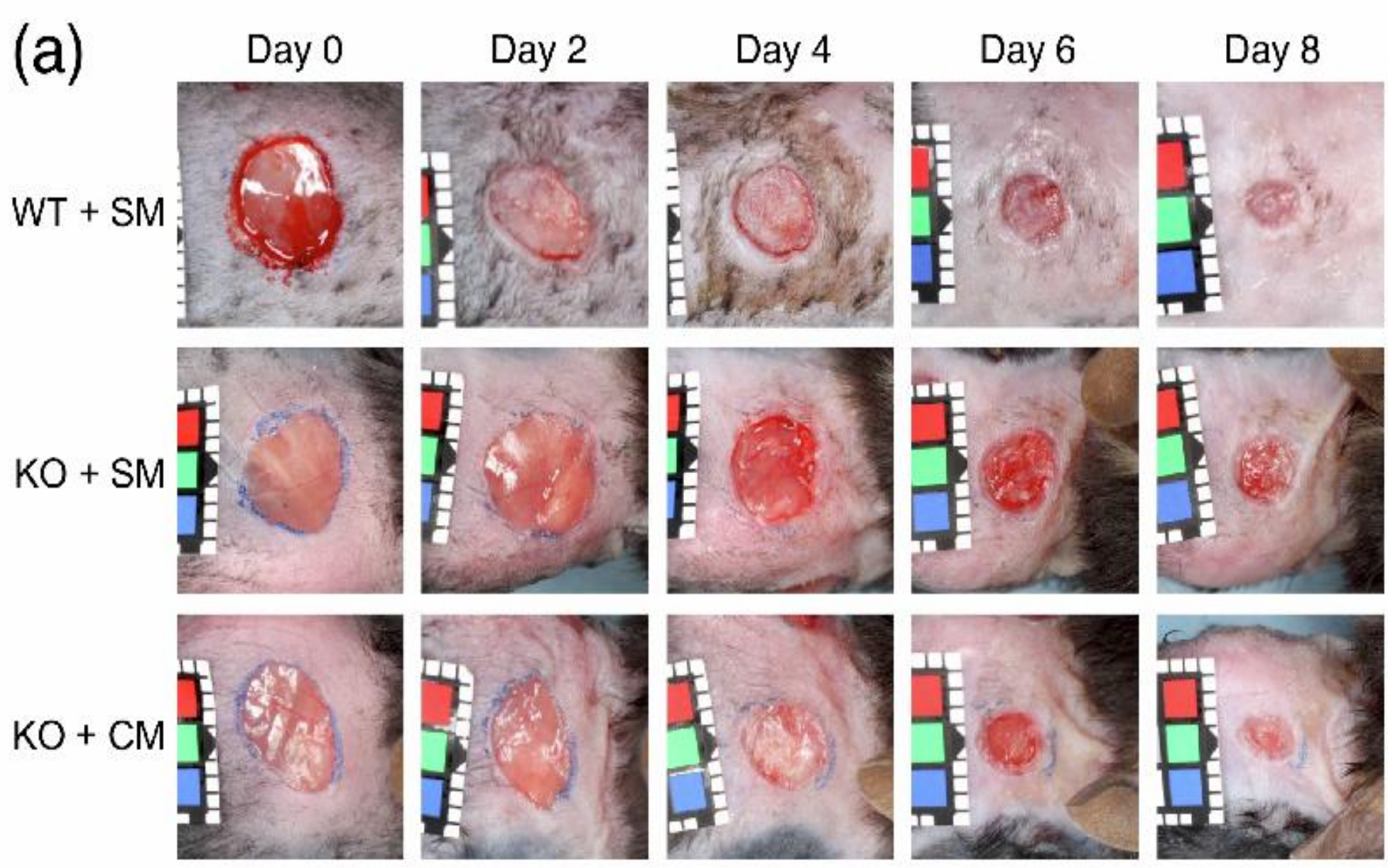
(a)
Day 0
Day 2
Day 4
Day 6
Day 8
WT + SM
KO + SM
KO + CM

(b)

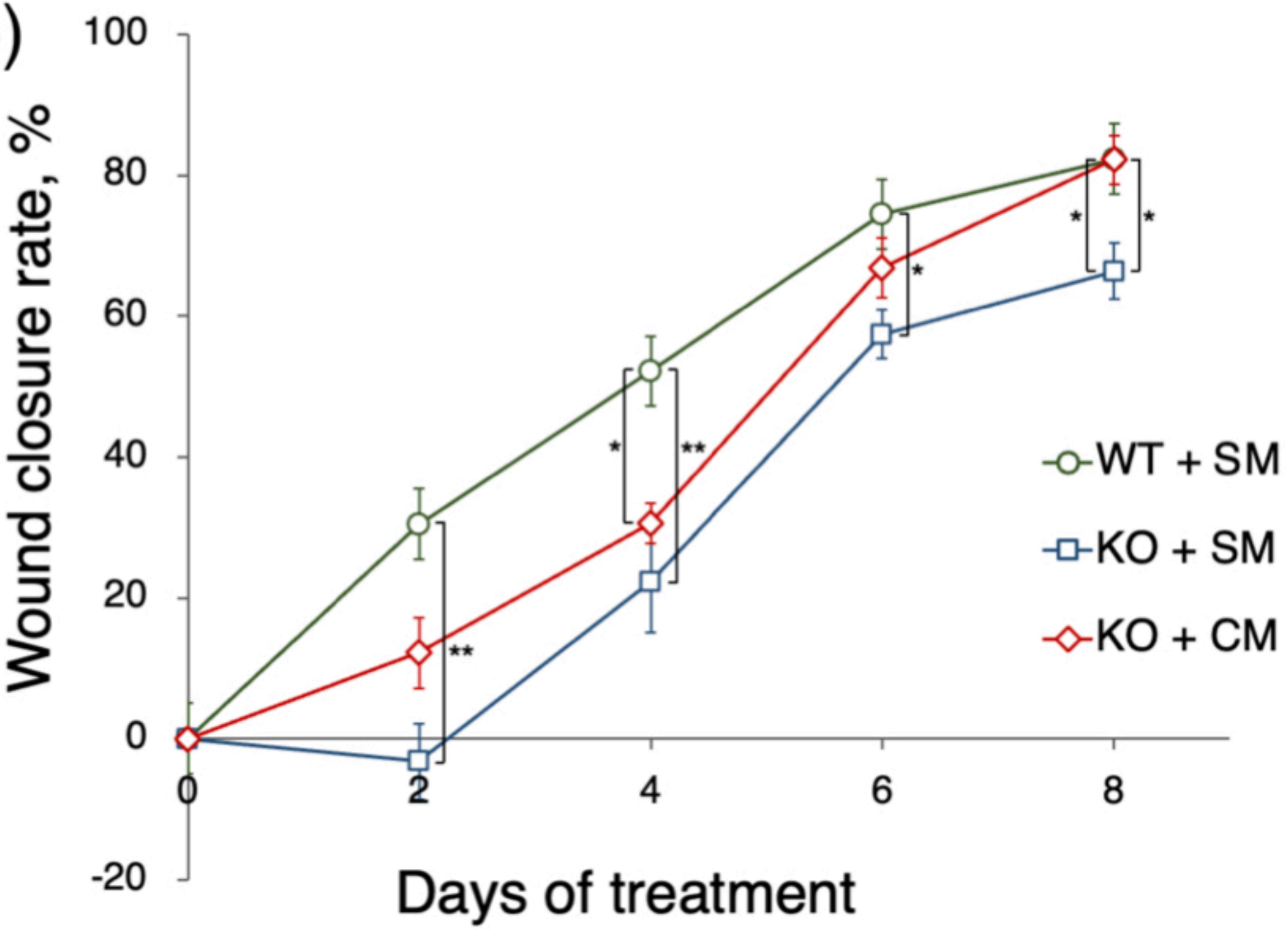
Wound closure rate, %
100
80
60
40
20
0
-20
0
2
4
6
8
Days of treatment
WT + SM
KO + SM
KO + CM
*
**
*
*
*
**

Fig. 2b

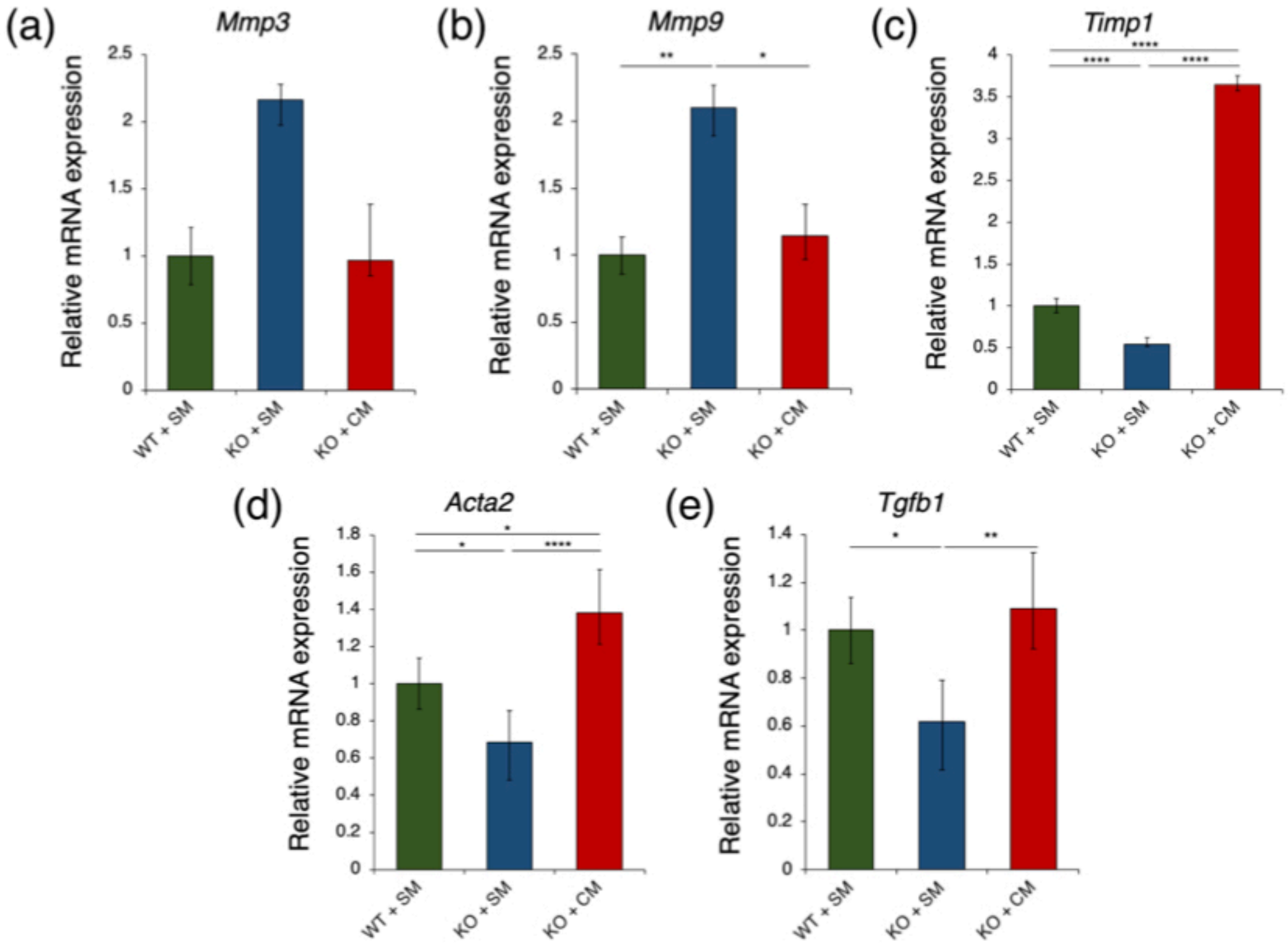
(a)
Mmp3
Relative mRNA expression
2.5
2
1.5
1
0.5
0
WT + SM
KO + SM
KO + CM
(b)
Mmp9
**
*
Relative mRNA expression
2.5
2
1.5
1
0.5
0
WT + SM
KO + SM
KO + CM
(c)
Timp1
****
****
****
Relative mRNA expression
4
3.5
3
2.5
2
1.5
1
0.5
0
WT + SM
KO + SM
KO + CM
(d)
Acta2
*
*
****
Relative mRNA expression
1.8
1.6
1.4
1.2
1
0.8
0.6
0.4
0.2
0
WT + SM
KO + SM
KO + CM
(e)
Tgfb1
*
**
Relative mRNA expression
1.4
1.2
1
0.8
0.6
0.4
0.2
0
WT + SM
KO + SM
KO + CM

Fig. 3

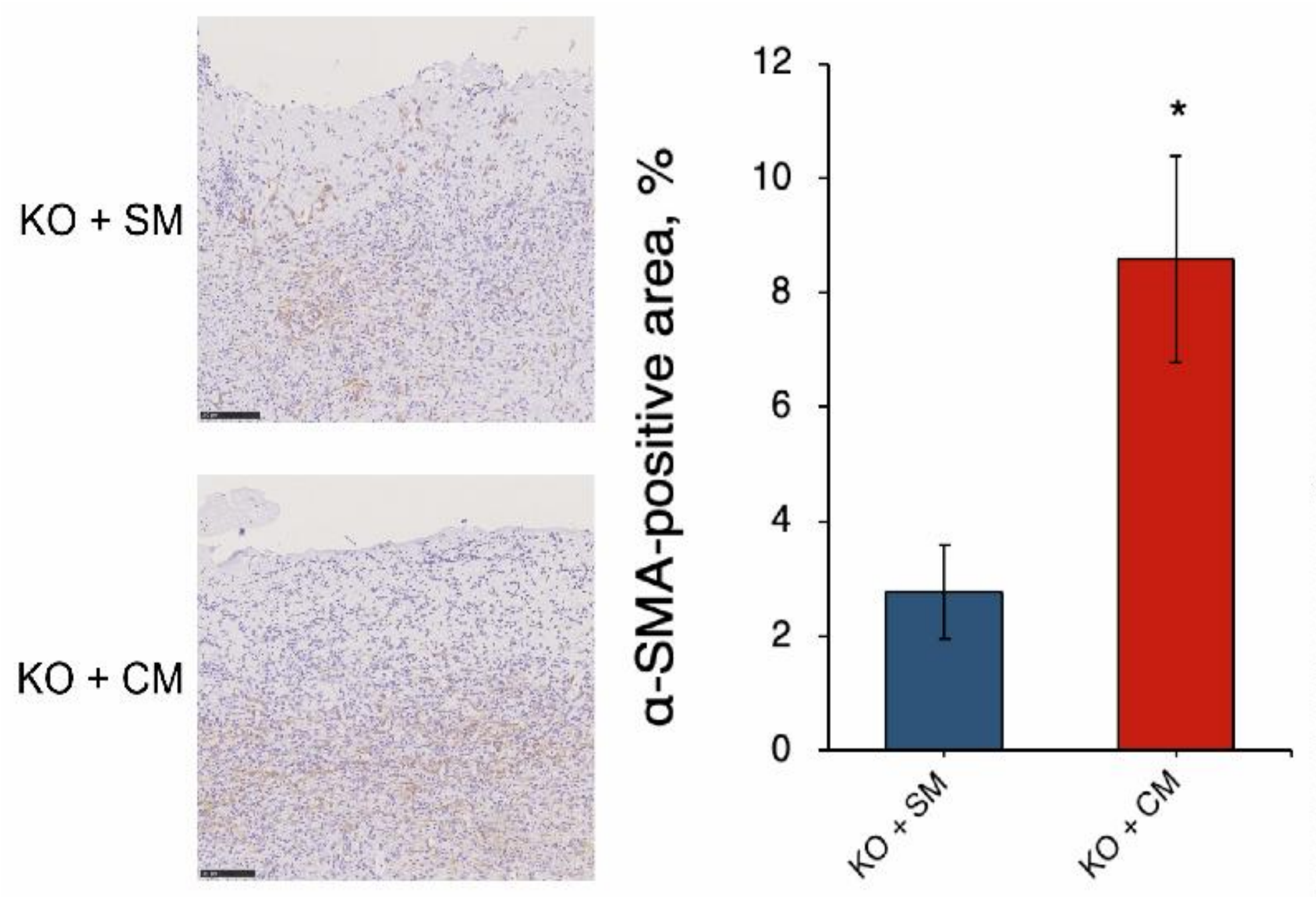
KO + SM
KO + CM
α-SMA-positive area, %
12
10
8
6
4
2
0
*
KO + SM
KO + CM

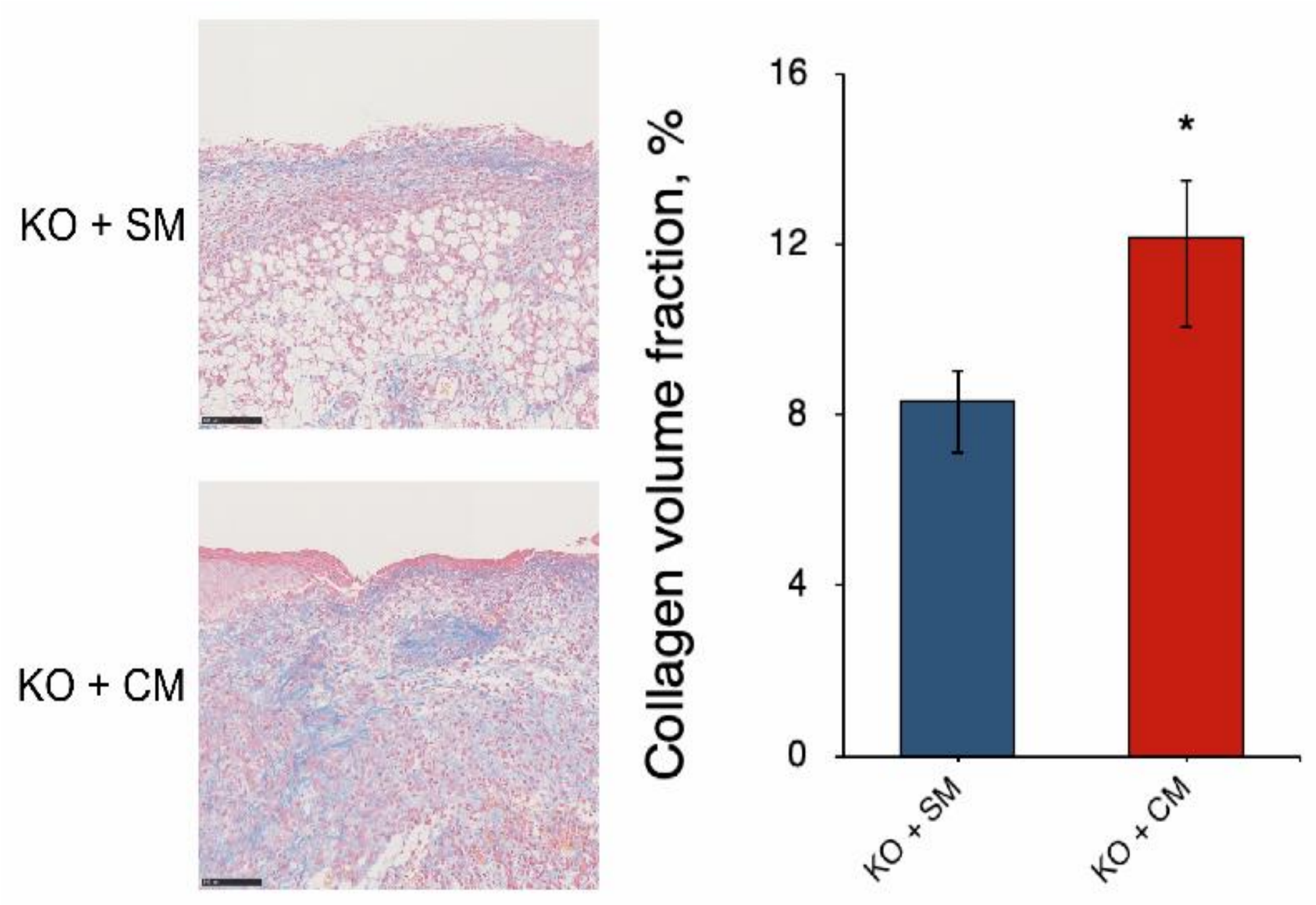
KO + SM
KO + CM
Collagen volume fraction, %
16
12
8
4
0
*
KO + SM
KO + CM

Supplementary Information

Extracellular matrix modulating effects of amnion-derived mesenchymal stem cells on aging skin wounds in α-Klotho knockout mice

Yuki Sasaki[1], Shunsuke Ohnishi [2], Hiroko Takahashi[1], Kosuke Ishikawa[1], Takahiro Miura[1], Emi Funayama[1], Naoto Okubo[2], Yuhei Yamamoto[1], Taku Maeda[1,*]

[1]Department of Plastic and Reconstructive Surgery, Faculty of Medicine and Graduate School of Medicine, Hokkaido University

[2]Laboratory of Molecular and Cellular Medicine, Faculty of Pharmaceutical Sciences, Hokkaido University

Table S1. Primer sequences.

Mouse *Acta2-forward*: 5′- GACAATGGGCTCTCTGGGCTCTCTGTA -3′

Mouse *Acta2-reverse*:5′- TTTGGCCCATTCCAACCATTA -3′

Mouse *Gapdh-forward*: 5′-TGTGTCCGTCGTGGATCTGA-3′

Mouse *Gapdh -reverse*: 5′-TTGCTGTTGAAGTCGCAGGAG-3′

Mouse *Il1b-forward*: 5′- CCAGGATGAGGACATGAGCAC-3′

Mouse *Il1b-reverse*:5′- TGTTGTTCATCTCTCGGGAGCCTGTA-3′

Mouse *Mki67-forward*: 5′- GCTCACCTGGGTCACCATCAA-3′

Mouse *Mki67-reverse*:5′- CACTACAGGCAGCTGGGATACGA-3′

Mouse *Mmp3-forward*: 5′- CCTGGGACCAGGGGATTAATGGGAG-3′

Mouse *Mmp3-reverse*: 5′- GGCCAAGTTCATGAGCAGCA-3′

Mouse *Mmp9-forward*:5′- GCCCTGGAACTCACACGACA-3′

Mouse *Mmp9-reverse*: 5′- TTGGAAACTCACACACGCCAGAAG-3′

Mouse *Pecam1-forward*: 5′- CCTCCAACAGAGCCAGCAGTA-3′

Mouse *Pecam1-reverse*:5′- CGATGACCACTCCAATGACAAC-3′

Mouse *Tgfb1-forward*: 5′- TTCAACACATCAGAGAGCTCCGAGA TG-3′

Mouse *Tgfb1-reverse*:5′- GTATCGCCAGGAATTGTTGCTGTA -3′

Mouse *Timp1-forward*:5′- TCAAAGACCTATAGTGCTGGCTGTG -3′

Mouse *Timp1-reverse*: 5′- AAAGTGACGGGCTCTCTGGGTAGTCCTC -3′

Mouse *Tnf-forward*: 5′- GCCTCTTCTCATTCCTGCTTGTG -3′

Mouse *Tnf-reverse*:5′- TGATGAGAGGGAGGCCATTTG -3′

Mouse *Vegfa-forward*: 5′- AACCCATTCCTGGCCCTGA-3′

Mouse *Vegfa-reverse*:5′- GATCCACAAAGCATGCCATGTC-3′

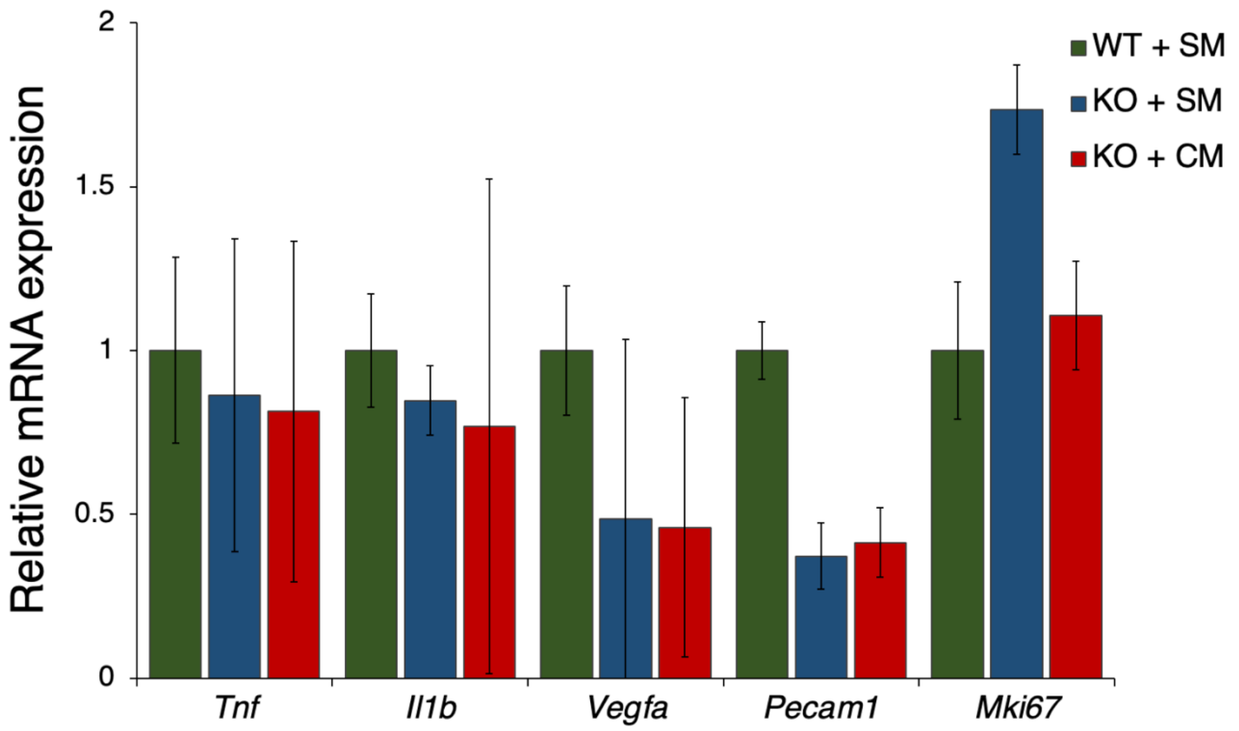

Figure S1.
Gene expression analysis of wound tissue at 8 days after wound ulcer creation. Wounds were created on the dorsum of wild-type (WT) mice or α-Klotho knockout (KO) mice, and standard medium (SM) gel or amnion-derived mesenchymal stem cells conditioned medium (CM) gel were applied topically every other day. On day 8, the mice were sacrificed, and ulcer tissue was collected. Data are shown as the mean ± standard error. n = 10 each. *WT*, wild-type mice; *SM*, standard medium; *KO*, α-Klotho knockout mice; *CM*, amnion-derived mesenchymal stem cell-conditioned medium; *Tnf*, tumor necrosis factor; *Il1b*, interleukin 1 beta; *Vegfa*, vascular endothelial growth factor a; *Pecam1*, platelet endothelial cell adhesion molecule 1; *Mki67*, marker of proliferation Ki-67.

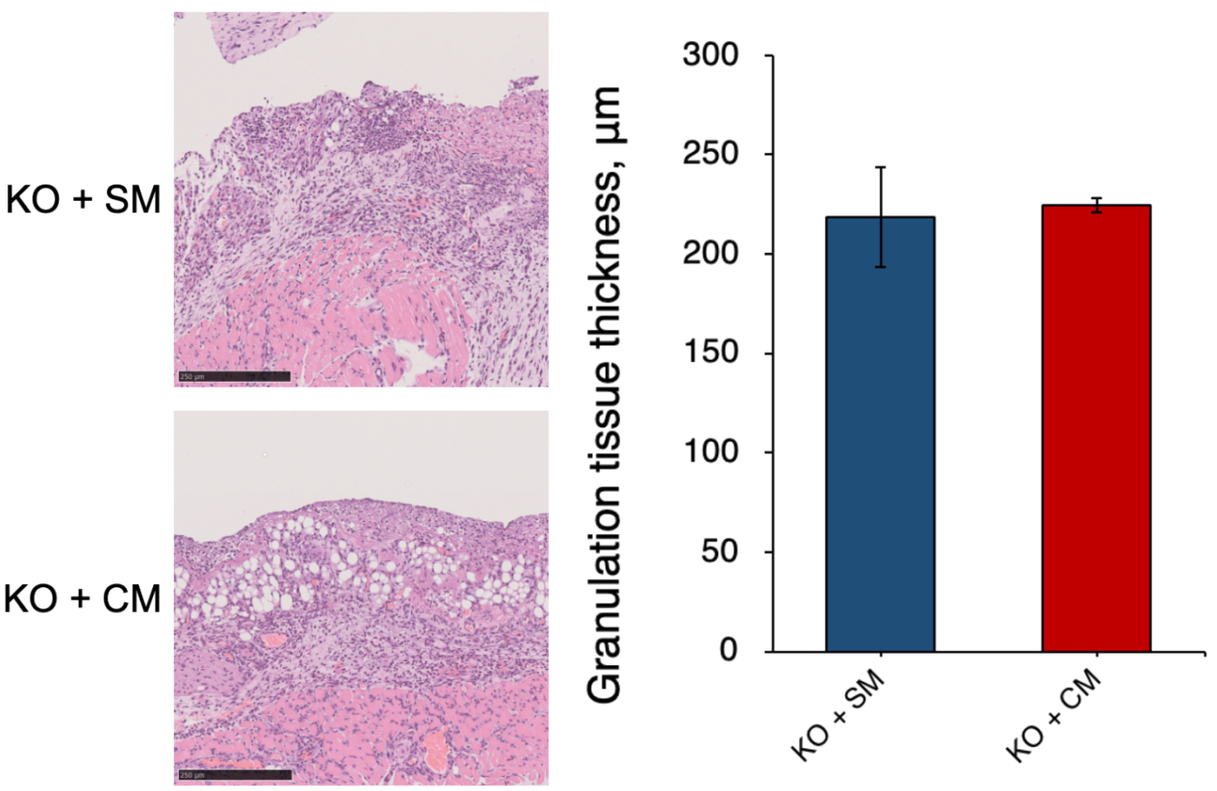

Figure S2.
Effect of amnion-derived mesenchymal stem cells on granulation tissue formation in wounds of α-Klotho knockout (KO) mice by hematoxylin and eosin staining. (Left) Microscopic images. (Right) Granulation tissue thickness. Data are shown as the mean ± standard error. *n* = 10 each. Scale bars = 250 μm.